Generalized Nash Bargaining Solution to Rate Control Optimization for Spatial Scalable Video Coding

Xu Wang, *Student Member, IEEE*, Sam Kwong, *Fellow, IEEE*, Long Xu, *Member, IEEE*, and Yun Zhang, *Member, IEEE*

***Abstract*— Rate control (RC) optimization is indispensable for scalable video coding (SVC) with respect to bitstream storage and video streaming usage. From the perspective of centralized resource allocation optimization, the inner-layer bit allocation problem is similar to the bargaining problem. Therefore, bargaining game theory can be employed to improve the RC performance for spatial SVC. In this paper, we propose a bargaining game-based one-pass RC scheme for spatial H.264/SVC. In each spatial layer, the encoding constraints, such as bit rates, buffer size are jointly modeled as resources in the inner-layer bit allocation bargaining game. The modified rate-distortion model incorporated with the inter-layer coding information is investigated. Then, the generalized nash bargaining solution (NBS) is employed to achieve an optimal bit allocation solution. The bandwidth is allocated to the frames from the generalized NBS adaptively based on their own bargaining powers. Experimental results demonstrate that the proposed RC algorithm achieves appealing image quality improvement and buffer smoothness. The average mismatch of our proposed algorithm is within the range of 0.19%–2.63%.**

***Index Terms*— Spatial scalable video coding, rate control, bargaining game, generalized nash bargaining solution, bargaining power.**

I. Introduction

With the rapid growth of network transmission capacity, enjoying video applications anytime and anywhere with various display terminals will be a desirable feature in the near future. For example, users may access the home video surveillance content by their smart phones with small resolution through the 4G LTE network, or replay it in their laptop with high definition (HD) display through the cables. To achieve the video streaming adaption under multiple terminals that are connected with different network configurations, a simple method is to encode the raw video several times with different settings. However, it is difficult for content providers to manage their huge of video streams. Another way is using transcoding techniques [1] but this kind of approach usually has a high computation complexity. To solve the problem posed by the characteristics of network transmission and application environment, the concept of scalability is introduced and supported in video compression, denoted as SVC [2]. The term scalability means that the terminals can decode from parts of the video stream to adapt it to the specific application requirements. In other words, SVC is an effective way to share and utilize the available bandwidth resources.

SVC has been investigated for more than two decades [3]. For example, the scalable bitstream is supported in the earlier international video coding standards such as MPEG-2, H.263 and MPEG-4. However, the scalable function will cause significant loss in coding efficiency and large increase in decoder complexity. Due to the lack of hardware computing power and limited bandwidth, these standards are not commercially successful. With the development of computation power of terminals and novel video tools such as the Hierarchical B-picture (HBP) structure and inter-layer prediction, H.264/SVC becomes a successful standardized scalable extension of H.264/AVC. In H.264/SVC, three kinds of scalability named spatial, temporal and quality scalability are supported in the bit stream according to the encoding configuration. For spatial SVC, the source video with high spatial resolution is downsampled with different spatial resolution. Then each SL is assigned with a fixed spatial resolution. For each SL, the HBP structure based temporal scalability and inter-layer prediction mechanisms are supported to improve the coding performance.

To adapt video stream to different channel bandwidth, terminal and user's requirement, RC plays an important role. It devotes to achieve a balance between visual quality and buffer smoothness under a given bandwidth constraint [4], [5]. For SVC, the video is usually encoded into bitstreams at

Manuscript received December 22, 2013; revised May 28, 2014; accepted July 11, 2014. Date of publication July 23, 2014; date of current version August 11, 2014. This work was supported in part by the Natural Science Foundation of China under Grant 61272289, Grant 61102088, and Grant 61202242, in part by the City University of Hong Kong Applied Research under Grant 9667094, in part by the Shenzhen Emerging Industries of the Strategic Basic Research Project under Grant JCYJ20120617151719115, in part by the Guangdong Nature Science Foundation under Grant S2012010008457, and in part by the City University of Hong Kong Shenzhen Research Institute, Shenzhen, China. The associate editor coordinating the review of this manuscript and approving it for publication was Dr. Joan Serra-Sagrista.

X. Wang and S. Kwong are with the Department of Computer Science, City University of Hong Kong, Hong Kong, and also with the City University of Hong Kong Shenzhen Research Institute, Shenzhen 5180057, China (e-mail: wangxu.cise@gmail.com; cssamk@cityu.edu.hk).

L. Xu is with the National Astronomical Observatories, Chinese Academy of Sciences, Beijing 100012, China, and also with the Department of Computer Science, City University of Hong Kong, Hong Kong (e-mail: lxu@jdl.ac.cn).

Y. Zhang is with the Shenzhen Institutes of Advanced Technology, Chinese Academy of Sciences, Shenzhen 518055, China, and also with the Department of Computer Science, City University of Hong Kong, Hong Kong (e-mail: yun.zhang@siat.ac.cn).

Color versions of one or more of the figures in this paper are available online at http://ieeexplore.ieee.org.

Digital Object Identifier 10.1109/TIP.2014.2341951

certain bit rates for storage although the SVC bitstreams can be decoded partially in decoder to achieve spatial, temporal or bit rate scalabilities [6]. In addition, to achieve compliant buffer constraint of video streaming, rate control is also needed for manipulating buffer constraint which was defined as hypothetic reference decoder (HRD) in both H.264/AVC and H.264/SVC. Thus, RC is indispensable for SVC with respect to bitstream storage and video streaming usage.

Existing bit allocation schemes for the spatial H.264/SVC mainly focus on the inter-layer bit allocation and inner-layer bit allocation. According to the application scenario of SVC, the target bit rate for the SLs are fixed or adaptively allocated. For the adaptive allocating scenario, the inter-layer bit allocation is employed to improve the system performance by adaptively allocate the bandwidth among different layers. Pranantha *et al.* [7] proposed a highly complex trellis-based scheme which can obtain a near-optimal solution compared to the full search algorithm. Since the inter-layer dependency relationship introduced by the inter-layer prediction is not well addressed, Liu *et al.* [8] investigated the dependency relationship between the base layer (BL) and enhancement layers (ELs) caused by the inter-layer prediction. They proposed a four-pass inter-layer bit allocation algorithm with good R-D performances. However, these two RC algorithms are time consuming due to the multi-pass encoding, which is more suitable for offline applications.

For the fixed allocating scenario, the target bandwidth for each SL is fixed. Therefore, the rate controller only needs to consider the inner-layer bit allocation. Several works on the one-pass bit allocation for HBP structure. For example, Xu *et al.* [10] proposed a scaling factor scheme to indicate the importance of different temporal levels (TLs) in the bit allocation scheme. Seo *et al.* [11] proposed a modified R-D model based on both the Variance Of Difference (VOD) and Mean Absolute Difference (MAD). Hu *et al.* [14] proposed a R-D model based on the linear quality dependency relationship and adaptively predicted the weighting factors to allocate bits efficiently among TLs. In spatial H.264/SVC, the lower SL is encoded before the higher SL for the same frame index. Therefore, the coding information of the lower SL is available to the higher SL, which might be helpful for further improvement on the R-D performance. Liu *et al.* [9] proposed a switchable MAD prediction algorithm, where the MAD information of the lower SL was adopted to predict the MAD of higher SL. Hu *et al.* [6] proposed a two-stage quantization parameter (QP) determination scheme by investigating the inter-layer information. In addition, the use of machine learning based algorithm is an interesting direction for mining the relationship between the coding information and objective function of RC scheme. For example, Sanz-Rodriguez *et al.* [15] proposed a novel variable bit rate (VBR) controller with radial basis function (RBF) network based QP estimation model to control the QP fluctuations. The model parameters are pre-trained and fixed during the implementation, in which the performance of algorithm may depend on the size of training set.

In this paper, the inner-layer bit allocation optimization of spatial H.264/SVC is investigated by introducing bargaining game theory. Firstly, the characteristics of the bit allocation problem are described as follows.

1) For the bit allocation of each SL, the frames in the same group of picture (GOP) compete for the limited resources (bandwidth, buffer size), which can be regarded as a **multi-player resource allocation problem**;
2) The inner-layer bit allocation should make a balance between system performance in terms of R-D performance, quality smoothness and buffer smoothness, which is also a **multi-objective optimization problem**.

Based on the above discussions, the inner-layer bit allocation problem is one special form of centralized resource allocation problem, which is similar to bargaining problem. Therefore, the process of inner-layer bit allocation can be modeled as bargaining games and solved by the corresponding axiomatic solutions. For video coding, the game theory based approach has shown its power on solving the bit allocation problem among the basic coding units. For the constant bit rate (CBR) RC optimization of MPEG4, the macroblock (MB) level and object level bit allocation problem were modeled as bargaining game [16] and an non-cooperate game [17], respectively. In our previous work [18], the bargaining game was employed for the frame level bit allocation of HBP structures of H.264/AVC. All the players (MBs/frames) in the bit allocation bargaining game [16], [18] are with equal bargaining power. These methods could improve the R-D performance of bit allocation. However, fairness problem [19] has not been fully addressed especially when the coding complexity of players are entirely different. As a variant of NBS, generalized NBS can improve the fairness by assigning players with different bargaining powers [19]. On the other hand, to exploit the coding redundancy, the inter-layer prediction technique is adopted in spatial H.264/SVC, which makes the R-D relationship different and hard to be estimated. At last, the buffer constraints are not concerned in the bargaining process. In this paper, the inner-layer bit allocation problem is modeled as bargaining game and solved by the generalized NBS. The major contributions of this paper are listed as follows.

1) Improve the R-D performance. To improve the prediction accuracy, guarantee the convexity of feasible utility set and reduce the computation complexity of solution, we investigate the R-D model by incorporating with the inter-layer coding information.
2) To guarantee the buffer smoothness, buffer constraints are modeled as lower and upper bound in the final optimization problem.
3) To improve the quality smoothness, the generalized NBS with adaptively determined bargaining powers is employed to obtain a closed-form solution in the optimization problem.

The rest of the paper is organized as follows. In Section II, the inner-layer bit allocation bargaining game is modeled. Section III provides the overall RC algorithms with parameter estimation and updating method. The experimental results based on H.264/SVC codec are provided in Section IV. Finally, Section V concludes the paper.

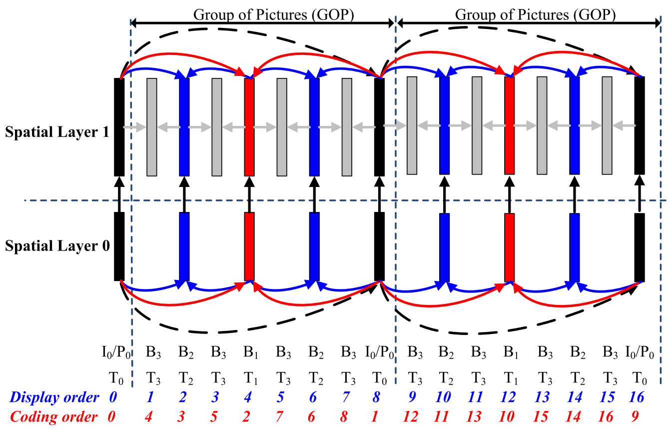

Fig. 1. Example of combined prediction structure within a GOP of H.264/SVC, where two spatial layers are shown.

II. Proposed Inner-Layer Bit Allocation Bargaining Game

In this section, the theoretical framework is firstly described for the inner-layer bit allocation bargaining problems of spatial H.264/SVC. Next, the utility function of players are defined based on the R-D model for the SLs. Finally, the generalized NBS is adopted to solve the bit allocation problem.

A. Inner-Layer Bit Allocation Bargaining Game

Bargaining is a type of negotiation in which players try to select one from many possible choices and eventually reach an agreement. The bargaining game models the bargaining interactions among players. In bargaining game, players compete for the limited resources and try to reach an agreement that has mutual benefits among them [19]. Each player has its own utility function to quantify its preference over the resources. If the total resources requested by players are less than the available, all the players' request are satisfied. Otherwise, the negotiation is compromised and all players will only obtain the minimum utility, named as disagreement point [20]. For spatial H.264/SVC, each SL has a limited bandwidth and buffer size, and it may not be able to assign satisfied bandwidth for all frames. As one kind of resource allocation problem, the inner-layer frame level bit allocation process is modeled as the bargaining game problem. Each frame-level rate controller of non-encoded frame in the same GOP is regarded as a player. For convenience, we assume that the total number of SL is L as shown in Fig. 1. For the SL s, total N_s players cooperate to divide the available bit rates R_c^s (remaining bits of the current GOP). The utility function of player j_s is denoted as $U_{j,s}(R_{j,s})$, where $R_{j,s}$ is the the number of allocated bits for the player j_s. During the bargaining game, each player will try to request for more bits to improve its image quality. Meanwhile, the player j_s will claim a minimum utility $d_{j,s}$ that can be derived from the bit rate $R_{j,s}^0$. In other words, the player j_s should be guaranteed a basic bit rate budget $R_{j,s}^0$. In addition, to avoid the buffer overflow or underflow, the number of bit allocated for the player j_s should be smaller than the maximum bandwidth budget or bigger than the minimum bandwidth budget, respectively. In this paper, the maximum bandwidth budget and minimum bandwidth budget is defined as $R_{j,s}^{\max}$ and $R_{j,s}^{\min}$, respectively. Given a combination of strategies carried out by all non-encoded frames $R_s = (R_{1,s}, R_{2,s}, \ldots, R_{N_s,s})$, then $U_s = (U_{1,s}(R_{1,s}), U_{2,s}(R_{2,s}), \ldots, U_{N_s,s}(R_{N_s,s}))$ is the corresponding utility of the game. Let that $\mathbf{d_s} = (d_{1,s}, d_{2,s}, \ldots, d_{N_s,s})$ be the disagreement point. Assume the feasible set $\mathbf{U_s} = \{U_s\} \subset \mathbb{R}^{N_s}$ is nonempty, convex, closed and bounded, then the pair $(\mathbf{U_s}, \mathbf{d_s})$ defines the bargaining problem for the SL s. To solve the bargaining game, the concept of Pareto Optimality is firstly defined as follows.

Definition 1 (Pareto Optimality [20]): The bit allocation point $U_s = (U_{1,s}, \ldots, U_{N_s,s}) \in \mathbf{U_s}$ is Pareto optimal if $V_s = U_s$ for each $V_s = (V_{1,s}, \ldots, V_{N_s,s}) \in \mathbf{U_s}$ with $V_s \geq U_s$.

Based on the properties of game, the bit allocation bargaining game with multiple players may contain numbers of Pareto optimal points. Therefore, we need a criterion for selecting the optimal Pareto optimality point, called the bargaining solution.

Definition 2 (Bargaining Solution [20]): A bargaining solution is a Pareto optimality point that satisfies the desired fairness axioms.

B. Rate Distortion Model Based Utility Function and Convexity

1) Rate Distortion Model for Spatial Layer: The utility function of players is defined based on the R-D model. To improve the R-D performance of RC problem, the most important thing is to build an accurate R-D model. In the literatures, many classical R-D models have been proposed. For example, analytical R-D models such as Cauchy distribution based model [21], quadratic model [22], Sum of Absolute Transform Differences (SATD) based model [23] and improved ρ-domain model [24], [25] had been widely investigated to enhance the accuracy of R-D relationship estimation. However, the R-D models are codec-specific. Therefore, we investigate the R-D model for spatial H.264/SVC.

In spatial H.264/SVC, the inter-layer prediction technique is introduced to exploit the coding redundancy, which makes the R-D characteristic different. Hence, we conduct experiments to exploit the R-D characteristics, where two SLs and four TLs are employed. The resolutions of the two layers for the sequences are CIF-4CIF or SD-HD. The sequences are encoded with various quantization step sizes denoted as Q_0 and Q_1 for the SLs 0 and 1, respectively. Firstly, we let $Q_0 = Q_1$ and encode the sequences with various Q_0 values. As shown in Fig. 2, the R-Q and R-D characteristics of frames in different TLs are different. For example, the number of bit rate of TL3 is smaller than that of the lower TL such as TL1 with the same QP value. The distortion in term of Mean Squared Error (MSE) for different TLs is also significantly different. On the other hand, the frames in the same TL have similar R-D characteristics. Therefore, each TL should have its own R-D model to reflect the coding complexity and quality preferences. As shown in (1), the quadratic based R-Q models are employed to achieve the bit allocation for their accuracy

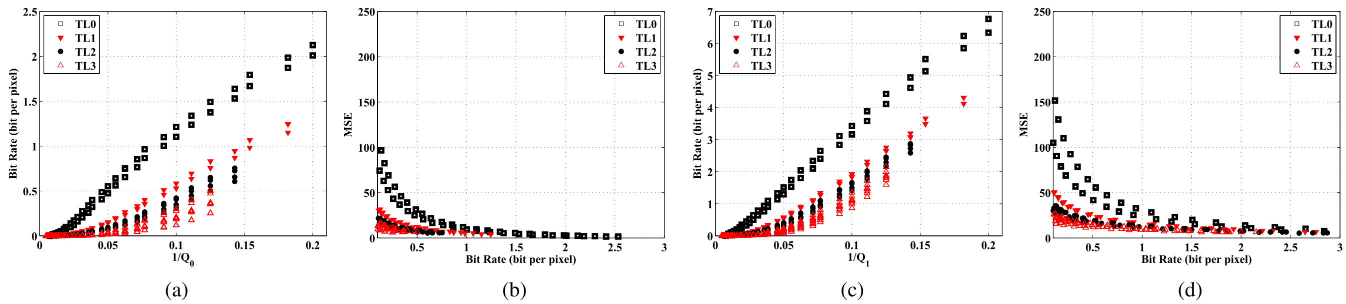

Fig. 2. R-D relationship for the pictures in TL0, TL1, TL2, and TL3 in Sequence "Harbour"(CIF-4CIF). (a) R_0 v.s. $1/Q_0$ of the SL 0; (b) D_0 v.s. R_0 of the SL 0; (c) R_1 v.s. $1/Q_1$ of the SL 1; (d) D_1 v.s. R_1 of the SL 1.

TABLE I
R-SQUARE OF CURVE FITTING RESULTS FOR R-Q MODEL

Type	Sequence	SL 0	SL 1
		(1)	(1)
4CIF	City	0.965	0.951
	Crew	0.987	0.951
	Harbour	0.979	0.962
	Soccer	0.996	0.968
HD	BasketballDrive	0.981	0.972
	BQTerrace	0.956	0.969
	Cactus	0.994	0.945
	Kimono1	0.991	0.909
	ParkScene	0.993	0.984
Average		**0.982**	**0.957**

and easy implementation.

$$R_{t,s} = \frac{\kappa_{t,s} \cdot m_{t,s}}{Q_{t,s}} + \frac{\nu_{t,s} \cdot m_{t,s}}{Q_{t,s}^2} + h_{t,s}, \quad (1)$$

where $\kappa_{t,s}$ and $\nu_{t,s}$ are the model parameters of the TL t in the SL t. The $m_{t,s}$ is the MAD value of of the TL t in the SL s. $h_{t,s}$ is the average header bits of the TL t in the SL s. As shown in Table I, the R-square values for the SL 0 and 1 are 0.982 and 0.957 in average, respectively. It indicates that using (1) can achieve accurate fitting result for different test sequences.

The Cauchy distribution based R-D models are also employed for defining the utility function as shown in (2).

$$D_{t,s} = \alpha_{t,s} \cdot R_{t,s}^{-\gamma_{t,s}}, \quad (2)$$

where $\gamma_{t,s}$ and $\alpha_{t,s}$ are the model parameters of the TL t in the SL s. To evaluate the fitting accuracy of proposed R-D model, experiments were conducted. As shown in Table II, the R-D model in (2) could achieve good R-square value except for the R-D relationship of the SL 1. The R-square value for the SL 1 is only 0.576 in average. In other words, the fitting results are unacceptable.

Due to the reference relationship between the SLs in H.264/SVC, the output bit rate and distortion of the SL s ($s > 0$) may depend on the QP of its reference layer. Therefore, the relationship between the SL s and its reference layer should be exploited to improve the accuracy of R-D model. In the experiments, we fix the Q_0 value and vary the Q_1 value. As shown in Fig. 3(a) and 3(b), the bit rates of the SL 1 is independent of the QP of the SL 0 when the QP of SL 1 is fixed. It indicates the QP of the SL 0 has little influence on the bit rate of the SL 1. That is the reason why the model (1) can achieve good performance for all the SLs. As shown in Fig. 3(c), the distortion of the SL 1 is influenced by the QP of the SL 0, particularly when the SL 0 is compressed with larger QP. The distortion dependency is caused by distortion propagation from the SL 0. Therefore, the R-D model for the SL s ($s > 0$) can be rewritten as follows.

$$D_{t,s}(Q_{t,s-1}, R_{t,s}) = \mathrm{f}_{t,s}(Q_{t,s-1}) \cdot R_{t,s}^{-\gamma_{t,s}}, \quad (3)$$

where $\mathrm{f}_{t,s}(\cdot)$ is a function of $Q_{t,s-1}$. In another experiment, we fix the Q_1 value and varied the Q_0 value. As shown in Fig. 3(d), when the Q_1 value of SL 1 is fixed, the relationship between the Q_0 of the SL 0 and the distortion of the SL 1 can be presented by a linear model. As the output rate of SL 1 increases (Q_1 value decreases), the slope of the linear model decreases. Then, we have

$$\mathrm{f}_{t,s}(Q_{t,s-1}) = \mu_{t,s} \cdot Q_{t,s-1} + b_{t,s}. \quad (4)$$

Therefore, the R-D models in (2) are modified as

$$D_{t,s} = \begin{cases} \alpha_{t,s} \cdot R_{t,s}^{-\gamma_{t,s}}, & s = 0 \\ (\mu_{t,s} \cdot Q_{t,s-1} + b_{t,s}) \cdot R_{t,s}^{-\gamma_{t,s}}, & s > 0 \end{cases} \quad (5)$$

where $\mu_{t,s}$ and $b_{t,s}$ are the model parameters of the TL t in the SL s. As shown in Table II, the R-square values for the SL 1 is 0.918 in average when (5) is adopted. Compared to the R-D model in (2), using (5) can improve the fitting accuracy. For the practical implementation of R-D model regression in one-pass RC algorithm, it is difficult to obtain an accurate estimation of parameter $\gamma_{t,s}$, which is sensitive to the disturbance. Traditional approaches are to fix or bound the $\gamma_{t,s}$ in a small range based on the prior knowledge. In this paper, we modified the (5) to make a balance between estimation accuracy and implementation simplicity.

$$D_{t,s} = \begin{cases} \alpha_{t,s} \cdot (R_{t,s} + c_{t,s})^{-1}, & s = 0 \\ (\mu_{t,s} \cdot Q_{t,s-1} + b_{t,s}) \cdot (R_{t,s} + c_{t,s})^{-1}, & s > 0 \end{cases} \quad (6)$$

where $c_{t,s}$ are the model parameters of the TL t in the SL s. The $\gamma_{t,s}$ is fixed as 1. As shown in Table II, the R-square values for the SL 0 and 1 are 0.951 and 0.898 in average, respectively. It indicates that the modified R-D model can achieve acceptable estimation accuracy.

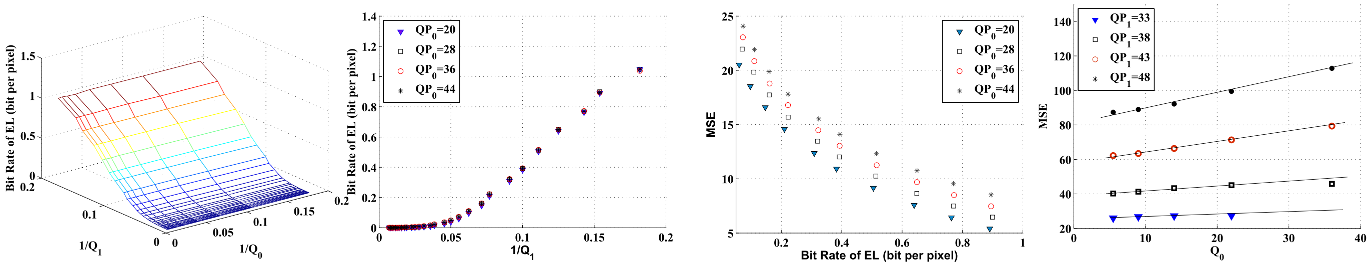

(a) (b) (c) (d)

Fig. 3. Dependent R-D relationship of the enhancement layer for the frame of in sequence "BQTerrace"(SD-HD). (a) R_1 v.s. Q_0 and Q_1; (b) R_1 v.s. Q_1 with fixed Q_0 value; (c) D_1 v.s. R_1 with fixed Q_0 value; (d) D_1 v.s. Q_0 with fixed Q_1 value.

TABLE II
R-SQUARE OF CURVE FITTING RESULTS FOR R-D MODEL

Type	Sequence	SL 0		SL 1		
		(2)	(6)	(2)	(5)	(6)
4CIF	City	0.959	0.931	0.667	0.872	0.866
	Crew	0.898	0.886	0.538	0.901	0.923
	Harbour	0.986	0.954	0.681	0.923	0.859
	Soccer	0.993	0.987	0.669	0.931	0.895
HD	BasketballDrive	0.988	0.957	0.387	0.915	0.946
	BQTerrace	0.963	0.923	0.887	0.946	0.916
	Cactus	0.997	0.994	0.543	0.916	0.934
	Kimono1	0.995	0.967	0.211	0.927	0.859
	ParkScene	0.990	0.962	0.598	0.935	0.886
Average		**0.974**	**0.951**	**0.576**	**0.918**	**0.898**

2) Definition of Utility Function: For video coding, the image quality is very important. Thus, we use the image quality to reflect the utility of each player. To define an effective utility function for one-pass rate control scheme, two criteria must be satisfied. First, we should guarantee the convexity of the feasible utility set. Second, the optimization problem can be solved with a closed form solution. Based on above-mentioned considerations, the utility function for the player j_s with TL index t is defined as

$$U_{j,s} = \frac{1}{D_{j,s}} = \frac{R_{j,s} + c_{t,s}}{\beta_{t,s}}, \tag{7}$$

where

$$\beta_{t,s} = \begin{cases} \alpha_{t,s}, & s = 0 \\ \mu_{t,s} \cdot Q_{t,s-1} + b_{t,s}, & s > 0. \end{cases} \tag{8}$$

$R_{j,s}$ is the allocated bits for the player j_s involved in the bit allocation game of SL s.

3) Convexity of Feasible Utility Set: In the bargaining problem, the properties of feasible utility set will influence the selection criteria of bargaining solution. Thus, we need to prove the convexity of feasible utility set.

Theorem 1: The feasible set $\mathbf{U_s}$ is a convex set.

Proof: From the definition of convex set, the feasible utility set $\mathbf{U_s}$ is convex if and only if for any utility point $X_s = (X_{1,s}, \ldots, X_{N_s,s}) = (U_{1,s}(x_s), \ldots, U_{N_s}(x_s))$, $Y_s = (Y_{1,s}, \ldots, Y_{N_s,s}) = (U_{1,s}(y_s), \ldots, U_{N_s}(y_s)) \in \mathbf{U_s}$ and any θ with $0 \le \theta \le 1$, s. t. $\theta X_s + (1-\theta) Y_s \in \mathbf{U_s}$, where the $x_s = (x_{1,s}, x_{2,s}, \ldots, x_{N_s,s})$ and $y_s = (y_{1,s}, y_{2,s}, \ldots, y_{N_s,s})$ are the bit rate allocation strategies which satisfy the rate constraints. For every j, $R^{min}_{j,s} < x_{j,s} \le R^{max}_{j,s}$, $R^{min}_{j,s} < y_{j,s} \le R^{max}_{j,s}$, and $\sum_{j=1}^{N_s} x_{j,s} \le R^s_c$, $\sum_{j=1}^{N_s} y_{j,s} \le R^s_c$.

For any θ with $0 \le \theta \le 1$, the following inequality

$$\begin{aligned} &\sum_{j=1}^{N_s} (\beta_{t,s}(\theta X_{j,s} + (1-\theta) Y_{j,s}) - c_{t,s}) \\ &= \theta \sum_{j=1}^{N_s} (\beta_{t,s} X_{j,s} - c_{t,s}) + (1-\theta) \sum_{j=1}^{N_s} (\beta_{t,s} Y_{j,s} - c_{t,s}) \\ &\le \theta R^s_c + (1-\theta) R^s_c \\ &= R^s_c \end{aligned} \tag{9}$$

holds. Therefore, the feasible utility set $\mathbf{U_s}$ is convex. ■

C. Generalized Nash Bargaining Solution

Since the utility set $\mathbf{U_s}$ is convex and bounded, the NBS defined in the following is suitable for solving the bit allocation bargaining game.

Theorem 2: (**NBS**) [20] Let F_s be a function defined as $F_s : (\mathbf{U_s}, \mathbf{d_s}) \to \mathbb{R}^{N_s}$, the NBS is a unique bargaining solution $U^*_s = F_s(\mathbf{U_s}, \mathbf{d_s})$ to the bit allocation bargaining game if all the axioms below are satisfied, which can be described as

$$U^*_s = \arg \max_{U_s \in \mathbf{U_s}} \prod_{j=1}^{N_s} (U_{j,s} - d_{j,s}) \tag{10}$$

The axioms for a NBS are listed as follows.

1) Individual Rationality: $U_{j,s}^* \geq d_{j,s}$ for all player j_s.
2) Feasibility: $U_{j,s}^* \in \mathbf{U_s}$.
3) Pareto Optimality: U_s^* is Pareto optimal.
4) Independence of Irrelevant Alternatives. If $U_s^* \in \mathbf{V_s'} \subset \mathbf{U_s}$, then $U_s^* = F_s(\mathbf{U_s}, \mathbf{d_s})$ derives $U_s^* = F_s(\mathbf{V_s'}, \mathbf{d_s})$.
5) Independence of Linear Transformations.
6) Symmetry.

The axioms 1-3 guarantee the existence and efficiency of the NBS, while the axioms 4-6 guarantee the fairness of the solution. The symmetry axiom guarantees the equal priority of users during the bargaining game when the users have the same utility functions and minimum utilities [19]. If the symmetry axiom is satisfied, then all the players involved in the bargaining game will be assigned the same bargaining powers. It may not be reasonable when the quality preference of players are significantly different. The generalized NBS [19], [26] is a variant of the NBS by assigning players with different bargaining powers. The objective function in (10) is modified as

$$U_s^* = \arg \max_{U_s \in \mathbf{U_s}} \prod_{j=1}^{N_s} (U_{j,s} - d_{j,s})^{w_{j,s}}, \tag{11}$$

where $w_{j,s}$ is the the corresponding bargaining power of player $j_{t,s}$.

Based on the previous proof and definition, the solution $U_s^* = U_s(R_s^*)$ is an generalized NBS of the SL s if and only if

$$\prod_{j=1}^{N_s} (U_{j,s}(R_{j,s}^*) - d_{j,s})^{w_{j,s}} \geq \prod_{j=1}^{N_s} (U_{j,s}(R_{j,s}) - d_{j,s})^{w_{j,s}}$$

for all $U_s \in \mathbf{U_s}$. Therefore, we can solve the following optimization problem (12) to obtain the generalized NBS.

$$\begin{aligned} &\max_{R_s} \prod_{j=1}^{N_s} (U_{j,s}(R_{j,s}) - d_{j,s})^{w_{j,s}} \\ &\qquad s.t. R_{j,s}^{\min} < R_{j,s} \leq R_{j,s}^{\max}, \\ &\qquad \sum_{j=1}^{N_s} R_{j,s} \leq R_c^s, \quad j = 1, \ldots, N_s. \end{aligned} \tag{12}$$

It is easy to prove that the optimization objective function (12) is concave. Based on the log-convexity properties of the objective function, the problem can be transformed as

$$\begin{aligned} &\max_{R_s} \sum_{j=1}^{N_s} w_{j,s} \cdot \ln(U_{j,s}(R_{j,s}) - d_{j,s}) \\ &\qquad s.t. R_{j,s}^{\min} < R_{j,s} \leq R_{j,s}^{\max}, \\ &\qquad \sum_{j=1}^{N_s} R_{j,s} \leq R_c^s, \quad j = 1, \ldots, N_s. \end{aligned} \tag{13}$$

Since the transformed problem is convex, the optimal solution can be obtained by solving the Karush-Kuhn-Tucker (KKT) conditions. Suppose the λ_s, $\theta_{j,s}$, and $\tau_{j,s}$ are the Lagrange multipliers, then we have the following Lagrangian function $L(R_{j,s}, \lambda_s, \theta_{j,s}, \tau_{j,s})$,

$$\begin{aligned} L = &\sum_{j=1}^{N_s} w_{j,s} \ln(U_{j,s}(R_{j,s}) - d_{j,s}) + \lambda_s \cdot (R_c^s - \sum_{j=1}^{N_s} R_{j,s}) \\ &+ \sum_{j=1}^{N_s} \theta_{j,s} \cdot (R_{j,s} - R_{j,s}^{\min}) + \sum_{j=1}^{N_s} \tau_{j,s} \cdot (R_{j,s}^{\max} - R_{j,s}). \end{aligned} \tag{14}$$

The KKT conditions of (14) are written as follows

$$\begin{cases} \frac{\partial L}{\partial R_{j,s}} = w_{j,s} \frac{\partial \ln(U_{j,s} - d_{j,s})}{\partial R_{j,s}} + (\theta_{j,s} - \lambda_s - \tau_{j,s}) = 0 \\ \frac{\partial L}{\partial \lambda_s} = R_c^s - \sum_{j=1}^{N_s} R_{j,s} \geq 0 \\ \lambda_s (R_c^s - \sum_{j=1}^{N_s} R_{j,s}) = 0 \\ \theta_{j,s} \cdot (R_{j,s} - R_{j,s}^{\min}) = 0 \\ \tau_{j,s} \cdot (R_{j,s}^{\max} - R_{j,s}) = 0 \end{cases} \tag{15}$$

where $j \in 1, \ldots, N_s$. Based on the above KKT conditions (15), we have

$$\begin{aligned} \frac{\partial L}{\partial R_{j,s}} &= w_{j,s} \cdot \frac{\partial \ln(U_{j,s} - d_{j,s})}{\partial R_{j,s}} - \lambda_s \\ &\Rightarrow R_{j,s} = \frac{w_{j,s}}{\lambda_s} + \beta_{t,s} d_{j,s} - c_{t,s}. \end{aligned} \tag{16}$$

and then

$$\begin{aligned} &R_c^s - \sum_{j=1}^{N_s} R_{j,s} = 0 \\ &\quad \Rightarrow \frac{1}{\lambda_s} = R_c^s - \sum_{j=1}^{N_s} (\beta_{t,s} d_{j,s} - c_{t,s}). \end{aligned} \tag{17}$$

Therefore,

$$R_{j,s} = \max(R_{j,s}^{\min}, \min(\frac{w_{j,s}}{\lambda_s} + \beta_{t,s} d_{j,s} - c_{t,s}, R_{j,s}^{\max})). \tag{18}$$

Finally, the optimal quantization step size for the player $j_{t,s}$ is determined by

$$Q_{j,s} = \frac{2 \nu_{t,s} m_{t,s}}{\sqrt{\kappa_{t,s}^2 m_{t,s}^2 + 4 \nu_{t,s} m_{t,s} (R_{j,s} - h_{t,s})} - \kappa_{t,s} m_{t,s}}. \tag{19}$$

III. Proposed Overall Rate Control Algorithm

In this section, the details of proposed rate control algorithm are described. Firstly, we introduce the estimation of the model parameters involved in the bit allocation bargaining game. Then the overall algorithm is provided.

A. Parameters Determination of Bargaining Game

To obtain a generalized NBS of the inner-layer bit allocation bargaining game, the model parameters should be determined first.

1) Parameters Determination of R-D Model: For the SL s, all the model parameters are unavailable before the first frame of TL t is encoded. In this paper, we use the same method in [18] to initialize the parameters of TL t. Once the frame located in TL t is encoded, the R-D model parameters such as $\kappa_{t,s}$, $h_{t,s}$ and $\alpha_{t,s}$ are updated by using the linear regression technique.

2) Parameters Determination of Bargaining Game: Before the optimal allocation result from (18), the parameters $d_{j,s}$ and $\beta_{j,s}$ for the SL s can be computed. The prediction of $d_{j,s}$ is based on the historical information of previously encoded frames that are located in the same TL. The estimation method is the same as in [18]. For the bargaining problem of SL $s > 0$ with N_s non-encoded frames, only the quantization step size $Q_{1,s-1}$ of the first frame in SL $s-1$ is known. Therefore, to predict the parameters $\beta_{j,s}$, we set $Q_{j,s-1}$ equal to $Q_{1,s-1}$ for $j = 2, \ldots, N_s$.

3) Adaptive Bargaining Powers Determination: As shown in (18), the bargaining powers can influence the bits allocation results. The bandwidth is divided into two parts. One part is used to guarantee the disagree point. If the bargaining powers are equal, then the remaining bandwidth will be allocated equally to each frame. Due to the difference of the utility functions among the frames in different TLs, the bargaining power $\omega_{j,s}$ for the player $j_{t,s}$ is determined as follows to achieve a fair bit allocation.

As shown in (6), the parameters $\beta_{t,s}$ determines the utility preference (i. e. coding complexity) of player $j_{t,s}$. Large value of $\beta_{t,s}$ indicates that the player $j_{t,s}$ will obtain smaller utility value than that of other players for the same number of bit rates. To ensure each player achieving similar utility, we let $\varphi_{j,s}$ be

$$\varphi_{j,s} = \frac{\beta_{j_t,s}}{\beta_{1_t,s}}. \tag{20}$$

The bargaining power $\omega_{j,s}$ is defined as

$$\omega_{j,s} = \frac{\varphi_{j,s}}{\sum_{i=1}^{N_s} \varphi_{i,s}}. \tag{21}$$

To explain the influence of bargaining powers on the algorithm performance, using the common PSNR value is more intuitive than direct using the utility of player. The relationship between Peak Signal-to-Noise Ratio (PSNR) and utility function is expressed as

$$\mathrm{PSNR}_{j,s} = 10 \cdot \log_{10}(255^2 \cdot U_{j,s}). \tag{22}$$

It is well known that the fairness axiom is satisfied for the generalized NBS. Thus, the generalized NBS with adaptive bargaining powers will reduce the utility difference among players. In other words, the quality smoothness is improved since the PSNR difference among players is reduced.

4) Buffer Management and Parameters Updating: Before encoding the frames in a GOP, the number of target bits for the SL s of current GOP [13] is firstly allocated as

$$R_c^s(n, 0) = \frac{B_s \cdot N_G^s}{F_s} + \gamma_s \cdot (\varsigma^s(n, 0) - \varsigma_T^s) \cdot B_u^s, \tag{23}$$

where $\varsigma^s(n, 0)$ indicates the buffer fullness status of the SL s when the the GOP $n-1$ is finished. ς_T^s is the target buffer fullness. N_G^s is the total number of frames in a GOP for the SL s. B_u^s is the buffer size. B_s is the target bandwidth and F_s is the frame rate. γ_s is the scale factor. In this paper, we let $\gamma_s = 0.5$. For the frame $j_{t,s}$ of the GOP n, the remaining target bits $R_c^s(n, j)$ for the rest frames is updated after obtaining the coding information of the frame j–1 [13] by using

$$R_c^s(n, j) = R_c^s(n, j-1) - R_o^s(n, j-1), \tag{24}$$

where $R_o^s(n, j-1)$ is the number of actual output bits of the frame $j-1$ in the GOP n.

Once a frame $j_{t,l}$ in the GOP n is encoded, the buffer fullness status $\varsigma^s(n, j)$ are also updated by

$$\varsigma^s(n, j) = \varsigma^s(n, j-1) + (B_s/F_s - R_o^l(n, j-1))/B_u^s, \tag{25}$$

where $s \geq l$. To avoid the buffer overflow and underflow, the constraints $R_{j,s}^{min}$ and $R_{j,s}^{max}$ are determined by

$$R_{j,s}^{\min} = \frac{B_s}{F_s} + (\varsigma_l - \varsigma^s(n, j)) \cdot B_u^s, \tag{26}$$

and

$$R_{j,s}^{\max} = \frac{B_s}{F_s} + (\varsigma_u - \varsigma^s(n, j)) \cdot B_u^s, \tag{27}$$

where ς_l and ς_u are the lower bound and upper bound of the buffer fullness status.

B. Overall Rate Control Algorithm

Our proposed algorithm is described in Table III.

TABLE III

PROPOSED OVERALL RATE CONTROL ALGORITHM

Step 1	Initialize the model parameters;
Step 2	Compute the total bit of the current GOP n of SL s by (23);
Step 3	For the current frame $j_{t,s}$ in the GOP n, determine the remaining target bits by (24) and generalized NBS in (18). Compute quantization step $Q_{j,s}$ for the current frame $j_{t,s}$ by (19);
Step 4	Perform encoding for the frame $j_{t,s}$ with the obtained $Q_{j,s}$ of Step 3;
Step 5	Update the buffer status and model parameters. If the last frame of current GOP is not reached, go to Step 3;
Step 6	If the sequences ends, finish; else goto Step 2.

IV. Experimental Results

A. Simulation Setup

To evaluate the performance of our proposed RC algorithm, we implement the proposed algorithm in the reference software JSVM 9.15 [12] and test with various video sequences. The SVC Baseline Profile is set as default in the experiments. Table IV summarizes the key simulation parameters for the reference software. Other parameters are set as default. The experiment contains two types of sequences and corresponding SVC configurations. In Type I, two layers are of CIF-4CIF format with five video sequences (City, Crew, Soccer, Harbours and Ice). In Type II, the two layers are of SD-HD format with another seven video sequences (BasketballDrive, BQTerrace, Cactus, Kimono1, ParkScence,

TABLE IV
SUMMARY OF SIMULATION PARAMETERS

	4CIF	HD
Profile	Scalable Baseline Profile	
Base Layer Mode	AVC Compatible	
Intra Period	-1	
Reference Number	1	
GOP Size	8/16	
Frame Number	257	
Symbol Mode	CABAC	
Search Mode	4(FastSearch)	
BL Resolution	352*288	960*540
EL Resolution	704*576	1920*1080
Frame Rate	60	
Search Range	32	
ELSearchRange	2	
NumberReferenceFrames	1	
FastBiSearch	1	

TABLE V
SUMMARY OF TEST RATE POINTS

Rate Points (kbps)	City	Crew	Harbour	Soccer/Ice	HD
512/1536	✓				
768/2304	✓	✓	✓	✓	
896/2688	✓				
896/2944				✓	
1024/3072	✓	✓	✓		
1280/3840		✓	✓	✓	✓
1536/4608		✓	✓	✓	
2560/7680					✓
5120/15360					✓
7680/23040					✓

WestWindEasy and SpeedBag). Layer 0 is the BL encoded without inter-layer prediction. Layer 1 is the SL using adaptive inter-layer prediction from the SL 0. All the key frames in the video sequence are encoded as P frames except for the first frame which is encoded as I frame. To evaluate the robustness of our proposed algorithm on GOP size, both GOP sizes of 8 and 16 are tested. The initial QP value is set default as in [12]. For each sequences, four different rate points are tested. The detailed information of rate points are summarized in Table V.

To make a fair performance comparison, the RC algorithms JVT-W043 [13] (denoted as W043), Hu's scheme [14] (denoted as Hu2012), Wang's scheme [18] (denoted as GT) and FixedQP tool are also implemented as benchmark. The W043 algorithm is extended to support the SL rate control, although the original version in JSVM only supported BL rate control. The multiple-pass algorithm FixedQP tool implemented in the JSVM software applies the logarithmic search algorithms to find the optimal QP. The FixedQP tool uses different QPs to encode the video sequence until the mismatch of BR is acceptable or the number of iterations exceeds its maximum value. In our experiments, the maximum mismatch is set as 2% and the number of maximal iterations for each layer is set as 10. Furthermore, our proposed algorithm is tested with equal bargaining powers (denoted as Proposed-EBP) and adaptive bargaining powers (denoted as Proposed-ABP).

B. Accuracy of Bit Rate Achievement

The accuracy of bit rate achievement is the basic criterion to evaluate the performance of RC algorithms. In this paper, we measure the accuracy of bit rate achievement by using the following equation

$$E = \frac{|R_t - R_o|}{R_t} \times 100\%, \tag{28}$$

where R_t and R_o are the target BR and actual output BR, respectively. The results of BR mismatch E (%) for all the RC algorithms are provided in Tables VI and VII.

As shown in Table VII, the mismatch of JVT-W043 is quite large which is larger than 10% in average for all the sequences when the GOP size is 16. Although the JVT-W043 algorithm has been adopted in the JSVM software as a reference tool, the performance is not effective enough. The mismatch of FixedQP tool depends on the setting of the maximum negative and positive mismatch and the number of maximal iterations. As shown in the Tables VI and VII, our proposed algorithm can achieve the best accuracy. The average mismatch of our proposed algorithm is within the range 0.19%–2.63%.

C. R-D Performance

To evaluate the R-D performance of the RC algorithms, the BDPSNR (dB) and BDBR(%) [28] are employed in our experiments for fair comparison. We set the algorithm W043 as the benchmark among the algorithms, then the performances of Hu2012 [14], GT [18], the proposed algorithm and the FixedQP tool are compared with algorithm W043 in terms of BDPSNR and BDBR. The results are summarized in Tables VIII and IX. The positive BDPSNR results or the negative BDBR results provided in the table mean that the R-D performance of the corresponding RC algorithm is better than that of algorithm W043. As shown in Tables VIII and IX, the FixedQP tool achieves the best R-D performance among all the RC algorithms for all kinds of video sequences, where the gains are obtained from the cascading QP setting. However, the QP setting is fixed for the whole sequence, which may cause the buffer overflow or underflow. In addition, the FixedQP tool is not suitable for real-time application due to the multiple-pass implementation. As observed from the results, our proposed algorithm can get more gains of performance among the one-pass RC schemes. Comparing with the GT algorithm, our proposed algorithm with ABP setting can improve the R-D performance from 0.10 to 0.16 dB in average. For better observation, six R-D curves are plotted in Figs. 4 and 5, where it can be seen that our proposed algorithm with adaptive bargaining powers are better than the other four one-pass RC schemes. From the results in Tables VIII and IX, we can see that the R-D performance of our proposed algorithm with ABP setting is better than that of EBP setting in most cases. In the offline resource allocation situation, the model parameters are pre-determined. The performance of the EBP is always larger than that of the ABP based on the definition of generalized NBS. But for the one-pass RC, the mode parameters are predicted from the coding history, which is sensitive to the regression error and noise disturbance.

TABLE VI

PERFORMANCE OF THE RC ALGORITHMS FOR THE TWO LAYERS IN TERMS OF STANDARD DEVIATION OF PSNR AND ACCURACY OF BIT RATE ACHIEVEMENT (GOPSIZE 8)

Type	Sequences	Layer	W043		Hu2012		GT		Proposed-EBP		Proposed-ABP		FixedQP	
			STD (dB)	E (%)	STD (dB)	E (%)	STD (dB)	E (%)	STD (dB)	E (%)	STD (dB)	E (%)	STD (dB)	E (%)
4CIF	City	0	3.48	4.43	1.48	1.70	1.79	0.68	1.72	0.48	1.58	0.37	0.88	1.03
		1	1.86	3.87	1.23	2.78	1.50	0.83	1.29	0.81	1.14	0.87	0.67	1.89
	Crew	0	3.98	3.16	2.30	2.04	2.16	0.47	2.11	0.75	2.11	0.58	1.28	1.26
		1	2.33	8.59	1.63	2.72	1.67	0.40	1.49	0.80	1.54	0.88	1.12	1.93
	Harbour	0	1.98	3.87	1.71	1.77	1.88	1.99	1.59	1.51	1.42	0.95	1.05	1.78
		1	1.73	3.96	1.10	2.47	1.61	1.09	1.07	0.57	0.88	0.87	0.97	2.78
	Ice	0	3.93	11.46	1.90	1.23	2.16	0.52	2.16	0.45	1.82	0.29	1.09	1.28
		1	4.96	9.61	1.42	1.72	1.49	0.62	1.46	0.77	1.30	0.66	0.84	0.89
	Soccer	0	2.69	5.03	2.20	2.46	2.22	0.37	2.23	0.46	1.98	0.28	1.26	1.04
		1	2.91	6.31	2.40	3.04	2.91	0.87	2.50	0.28	2.33	0.47	1.54	1.71
HD	BasketballDrive	0	2.19	5.28	1.50	1.49	1.70	0.83	1.45	0.26	1.40	0.19	1.03	1.05
		1	1.28	5.30	1.32	1.77	1.25	0.40	1.12	0.39	1.03	0.39	0.84	1.02
	BQTerrace	0	2.86	5.69	2.21	1.37	2.09	1.27	1.93	0.75	1.81	0.40	1.10	1.27
		1	1.76	4.26	1.67	1.42	1.40	0.93	1.27	0.48	1.22	1.35	0.81	2.28
	Cactus	0	2.72	6.23	1.09	1.35	1.72	0.66	1.46	0.14	1.30	0.14	0.62	1.16
		1	1.49	5.80	1.01	1.51	1.19	2.18	0.98	1.07	0.92	1.87	0.53	3.27
	Kimono1	0	2.90	0.68	2.52	1.42	2.90	0.81	2.76	0.42	2.63	0.36	0.96	1.75
		1	1.73	1.31	1.67	1.49	1.69	1.50	1.30	0.90	1.27	0.58	0.68	1.63
	ParkScene	0	2.72	4.13	1.10	1.20	1.46	0.72	1.26	1.15	1.14	0.98	0.65	1.08
		1	1.71	4.63	1.04	1.74	1.20	1.42	1.00	1.47	0.90	1.08	0.52	1.95
	WestWindEasy	0	3.10	22.34	1.82	1.41	2.36	0.20	2.23	0.19	2.21	0.35	1.03	1.41
		1	2.01	10.10	1.47	1.58	1.55	0.28	1.34	0.32	1.36	0.52	1.09	1.36
	SpeedBag	0	1.98	2.99	2.25	1.40	2.11	1.55	1.37	1.08	1.53	2.63	1.24	0.77
		1	2.24	3.37	1.75	1.82	2.42	3.86	1.68	1.00	1.66	1.67	1.42	0.94
	Average	0	**2.88**	**6.27**	**1.84**	**1.57**	**2.05**	**0.84**	**1.85**	**0.64**	**1.74**	**0.63**	**1.02**	**1.24**
		1	**2.17**	**5.59**	**1.48**	**2.00**	**1.65**	**1.20**	**1.38**	**0.74**	**1.30**	**0.93**	**0.92**	**1.80**

TABLE VII

PERFORMANCE OF THE RC ALGORITHMS FOR THE TWO LAYERS IN TERMS OF STANDARD DEVIATION OF PSNR AND ACCURACY OF BIT RATE ACHIEVEMENT (GOPSIZE 16)

Type	Sequences	Layer	W043		Hu2012		GT		Proposed-EBP		Proposed-ABP		FixedQP	
			STD (dB)	E (%)	STD (dB)	E (%)	STD (dB)	E (%)	STD (dB)	E (%)	STD (dB)	E (%)	STD (dB)	E (%)
4CIF	City	0	5.35	4.60	2.15	4.30	2.13	1.59	2.17	0.73	1.96	0.47	1.10	1.24
		1	3.22	6.40	1.37	5.63	1.37	2.47	1.27	2.63	1.13	1.74	0.86	1.52
	Crew	0	3.32	11.72	2.61	6.41	2.27	0.77	2.20	1.77	2.03	1.17	1.41	0.86
		1	3.39	6.44	2.44	11.82	1.71	1.55	1.49	2.37	1.44	1.30	1.17	0.58
	Harbour	0	3.15	6.91	1.33	4.73	1.55	0.98	1.22	0.68	1.13	0.87	1.05	1.04
		1	2.89	12.11	1.73	8.11	1.27	0.66	1.13	1.21	1.03	0.64	0.97	1.20
	Ice	0	4.32	49.47	2.26	3.64	2.32	1.47	2.47	1.15	2.25	1.43	1.09	0.46
		1	3.59	39.27	2.21	6.64	1.86	1.64	1.97	2.43	1.79	2.01	0.85	0.88
	Soccer	0	4.50	7.15	2.05	5.92	2.46	0.95	2.28	0.79	2.17	0.12	1.32	1.24
		1	3.93	10.14	2.40	5.98	2.70	3.71	2.49	1.80	2.53	0.48	1.66	0.83
HD	BasketballDrive	0	3.24	18.14	1.72	2.73	1.69	0.72	1.42	0.68	1.36	0.76	1.09	1.20
		1	2.17	10.98	1.85	4.02	1.20	0.95	1.05	0.35	0.99	0.21	0.90	0.92
	BQTerrace	0	4.81	13.39	2.73	3.10	2.45	1.74	2.26	1.28	2.07	0.79	1.19	1.18
		1	2.83	6.12	2.12	5.63	1.39	1.29	1.31	1.03	1.24	0.84	0.90	1.30
	Cactus	0	4.13	15.98	1.48	4.33	1.71	0.82	1.57	0.50	1.41	0.39	0.74	1.65
		1	2.64	11.54	1.45	6.80	1.13	1.11	1.07	1.49	0.95	1.10	0.63	0.61
	Kimono1	0	3.92	6.71	2.75	4.36	2.92	1.97	2.74	1.88	2.65	0.65	1.14	0.53
		1	2.81	6.84	2.15	4.96	1.69	2.39	1.46	1.71	1.42	1.63	0.80	0.68
	ParkScene	0	3.94	13.57	1.49	4.13	1.88	1.38	1.64	1.48	1.50	0.24	0.82	2.29
		1	2.73	10.45	1.67	8.77	1.26	1.32	1.13	0.50	1.03	0.71	0.65	1.40
	WestWindEasy	0	4.36	6.43	2.29	4.05	2.73	0.93	2.26	1.71	2.24	1.21	1.07	0.86
		1	3.00	26.88	2.06	6.48	1.86	4.36	1.43	1.17	1.51	0.82	1.14	1.37
	SpeedBag	0	3.01	24.50	2.53	6.12	2.08	1.30	1.56	0.76	1.45	1.18	1.36	1.35
		1	3.10	22.12	2.07	7.69	2.06	1.60	1.75	1.64	1.69	0.39	1.43	1.42
	Average	0	**4.00**	**14.88**	**2.11**	**4.49**	**2.18**	**1.22**	**1.98**	**1.12**	**1.85**	**0.77**	**1.11**	**1.16**
		1	**3.03**	**14.11**	**1.96**	**6.88**	**1.63**	**1.92**	**1.46**	**1.53**	**1.40**	**0.99**	**1.00**	**1.06**

On the other hand, the ABP setting assigns more bits to the frames in the lower TLs comparing to the EBP setting. Due to the temporal dependency distortion relationship and distortion propagation, the R-D gain of the frames in the lower TLs might improve the R-D performance of the frames in the higher TLs.

D. Buffer Regulation and Quality Smoothness

In the experiments, the buffer size is set as $0.5B_s$, i.e., the maximum buffer delay is limited to $0.5s$. The initial buffer fullness and target buffer fullness are also set as 0.5 for all the SL. The lower bound ς_l and upper bound ς_u are set as

TABLE VIII
RESULTS FOR THE TWO LAYERS IN TERMS OF BDPSNR AND BDBR. (GOP SIZE: 8)

Type	Sequences	Layer	Hu2012		GT		Proposed-EBP		Proposed-ABP		FixedQP	
			BDPSNR (dB)	BDBR (%)	BDPSNR (dB)	BDBR (%)	BDPSNR (dB)	BDBR (%)	BDPSNR (dB)	BDBR (%)	BDPSNR (dB)	BDBR (%)
4CIF	City	0	0.16	-2.53	0.49	-11.74	0.49	-11.77	0.78	-25.36	0.96	-21.57
		1	0.03	-1.67	0.12	-9.92	0.14	-7.16	0.24	-8.99	0.46	-18.20
	Crew	0	0.42	-7.67	0.82	-14.86	0.90	-16.24	0.92	-16.52	1.10	-19.91
		1	0.20	-8.41	0.46	-15.44	0.61	-22.45	0.57	-21.70	0.75	-27.88
	Harbour	0	0.01	0.37	0.01	-6.23	0.12	-4.05	0.12	-4.25	0.47	-9.97
		1	0.05	-0.99	-0.02	-2.32	0.12	-3.80	0.24	-7.50	0.33	-10.24
	Ice	0	0.10	-1.59	0.40	-6.72	0.43	-7.19	0.58	-9.53	0.67	-11.26
		1	0.08	-0.66	0.33	-8.38	0.37	-9.83	0.40	-11.17	0.51	-14.17
	Soccer	0	0.10	-2.45	0.29	-5.43	0.24	-4.55	0.34	-6.39	0.56	-10.34
		1	0.09	-3.04	0.06	7.45	0.41	-11.59	0.46	-12.77	0.59	-17.27
HD	BasketballDrive	0	0.04	-0.41	0.31	-5.81	0.27	-4.87	0.34	-6.42	0.65	-11.96
		1	0.03	-1.07	0.17	-6.00	0.20	-6.85	0.27	-9.47	0.39	-13.44
	BQTerrace	0	0.05	-1.61	0.52	-14.01	0.49	-13.04	0.63	-16.90	1.00	-25.04
		1	0.01	-0.11	0.07	-3.12	0.13	-8.27	0.13	-10.13	0.36	-20.85
	Cactus	0	0.02	-0.54	0.24	-4.09	0.20	-4.06	0.25	-5.37	0.75	-14.28
		1	0.05	-3.03	0.17	-5.96	0.20	-7.14	0.19	-5.46	0.44	-19.61
	Kimono1	0	0.02	-0.15	0.11	-1.79	0.20	-3.92	0.25	-4.77	0.24	-4.15
		1	0.13	-3.38	-0.12	6.89	0.23	-4.03	0.25	-5.05	0.50	-11.74
	ParkScene	0	-0.08	2.23	0.44	-9.60	0.28	-5.71	0.42	-8.97	0.71	-13.82
		1	-0.03	0.98	0.23	-7.21	0.09	-2.76	0.25	-7.60	0.47	-13.04
	SpeedBag	0	-0.20	11.74	0.12	3.76	0.15	3.93	0.22	2.64	0.59	-4.11
		1	-0.10	3.27	0.22	-7.25	0.34	-9.62	0.36	-10.46	0.64	-19.62
	WestWindEasy	0	-0.34	9.79	0.01	-0.08	0.06	-1.39	0.05	-1.47	0.22	-5.34
		1	-0.32	7.73	-0.16	5.84	0.09	-1.92	0.11	-2.36	0.28	-5.95
	Average	0	**0.02**	**0.60**	**0.31**	**-6.38**	**0.32**	**-6.07**	**0.41**	**-8.61**	**0.66**	**-12.65**
		1	**0.02**	**-0.87**	**0.13**	**-3.79**	**0.24**	**-7.95**	**0.29**	**-9.39**	**0.48**	**-16.00**

TABLE IX
RESULTS FOR THE TWO LAYERS IN TERMS OF BDPSNR AND BDBR. (GOP SIZE: 16)

Type	Sequences	Layer	Hu2012		GT		Proposed-EBP		Proposed-ABP		FixedQP	
			BDPSNR (dB)	BDBR (%)	BDPSNR (dB)	BDBR (%)	BDPSNR (dB)	BDBR (%)	BDPSNR (dB)	BDBR (%)	BDPSNR (dB)	BDBR (%)
4CIF	City	0	0.20	-5.01	0.63	-16.53	0.81	-22.86	0.85	-23.32	1.54	-36.13
		1	0.06	-2.25	0.32	-11.29	0.38	-14.35	0.47	-16.31	0.80	-26.93
	Crew	0	0.24	-9.45	0.66	-18.98	0.69	-19.72	0.70	-20.23	0.90	-24.82
		1	0.07	-2.09	0.38	-12.79	0.43	-14.45	0.47	-15.93	0.63	-20.93
	Harbour	0	0.07	-1.78	0.39	-9.67	0.46	-10.98	0.50	-11.57	0.69	-16.07
		1	0.11	-2.18	0.44	-13.81	0.50	-14.94	0.46	-14.85	0.62	-19.41
	Ice	0	-0.28	5.96	0.32	-6.79	0.34	-7.05	0.43	-8.85	0.69	-13.58
		1	0.14	8.37	0.88	-8.39	1.02	-9.91	1.09	-11.66	1.32	-18.18
	Soccer	0	0.09	-2.39	0.27	-5.84	0.24	-5.40	0.32	-6.76	0.75	-14.37
		1	0.26	-6.25	0.51	-13.64	0.50	-16.17	0.57	-18.21	0.92	-30.97
HD	BasketballDrive	0	0.08	-0.26	0.52	-9.65	0.62	-11.35	0.63	-11.79	1.00	-17.82
		1	0.16	-7.61	0.48	-16.76	0.51	-17.06	0.53	-17.76	0.67	-22.08
	BQTerrace	0	0.66	-28.61	1.38	-30.98	1.44	-31.49	1.51	-36.54	1.98	-44.93
		1	0.10	-20.18	0.50	-37.48	0.57	-39.56	0.60	-42.69	0.78	-53.34
	Cactus	0	0.32	-6.85	0.69	-14.18	0.77	-15.37	0.91	-18.32	1.55	-27.93
		1	0.10	-12.47	0.35	-20.83	0.37	-19.35	0.43	-22.24	0.67	-30.89
	Kimono1	0	0.15	-3.88	0.41	-8.97	0.48	-10.86	0.46	-10.41	0.59	-12.52
		1	0.41	-8.49	0.91	-23.67	1.00	-22.19	1.05	-24.81	1.29	-32.34
	ParkScene	0	0.24	-12.73	0.99	-26.40	1.00	-26.12	1.09	-27.87	1.51	-33.72
		1	0.19	-1.08	0.66	-17.13	0.72	-18.11	0.82	-22.01	1.14	-26.95
	SpeedBag	0	-0.44	7.96	0.40	-8.72	0.65	-11.85	0.77	-14.18	1.42	-24.58
		1	-0.10	8.33	0.44	-3.80	0.73	-9.80	0.71	-10.94	1.07	-23.99
	WestWindEasy	0	-0.76	23.42	0.02	-1.23	0.06	-2.13	0.09	-2.79	0.34	-9.13
		1	-0.71	17.93	0.24	-6.73	0.22	-6.21	0.29	-7.80	0.48	-12.42
	Average	0	**0.05**	**-2.80**	**0.56**	**-13.16**	**0.63**	**-14.60**	**0.69**	**-16.05**	**1.08**	**-22.97**
		1	**0.07**	**-2.33**	**0.51**	**-15.53**	**0.58**	**-16.84**	**0.62**	**-18.77**	**0.87**	**-26.54**

0.1 and 0.9, respectively. As shown in Fig. 6, our proposed RC algorithm can prevent the buffer overflow and underflow. Note that the buffer smoothness and quality smoothness are not controlled very well for the beginning GOPs. There are two reasons. First, unoptimized initial QP setting [12] can cause drastic buffer fluctuation, especially for the larger mismatch between the target and output bit rates of the initial frame. Second, the accuracy of model parameters depends on the number of coded frames.

From Fig. 6, the buffer fullness status of our proposed algorithm can converge to the target buffer fullness as the number of encoded frames increases, which indicates the effectiveness of our proposed algorithms. For evaluating the quality smoothness, the standard deviation of PSNR defined in (29) is used

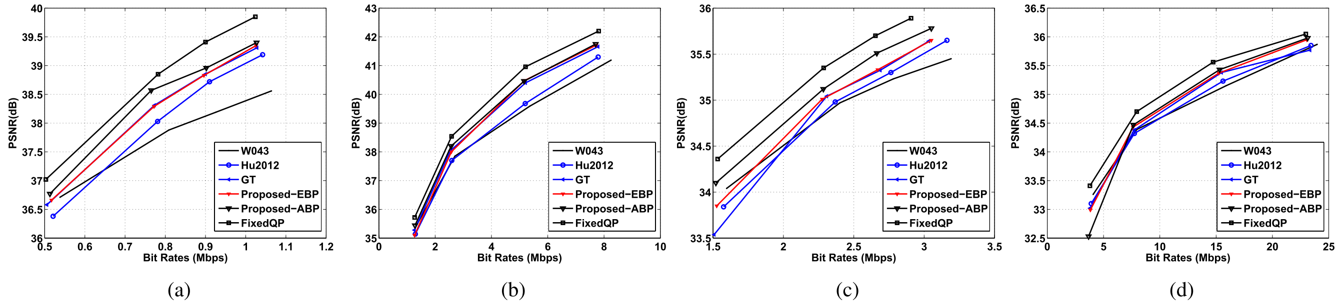

Fig. 4. R-D curves (GOP Size: 8). (a) SL 0: "City" (4CIF); (b) SL 0: "BQTerrace" (HD); (c) SL 1: "City" (4CIF); (d) SL 1: "BQTerrace" (HD).

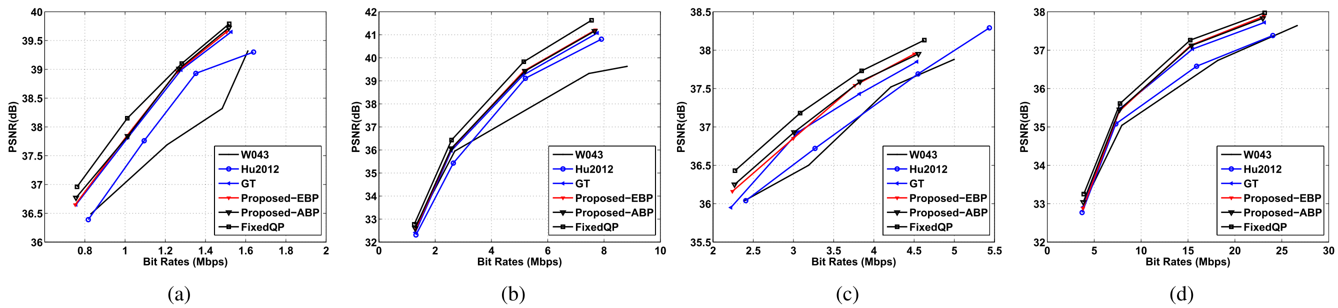

Fig. 5. R-D curves (GOP Size: 16). (a) SL 0: "Crew" (4CIF); (b) SL 0: "BasketballDrive" (HD); (c) SL 1: "Crew" (4CIF); (d) SL 1: "BasketballDrive" (HD).

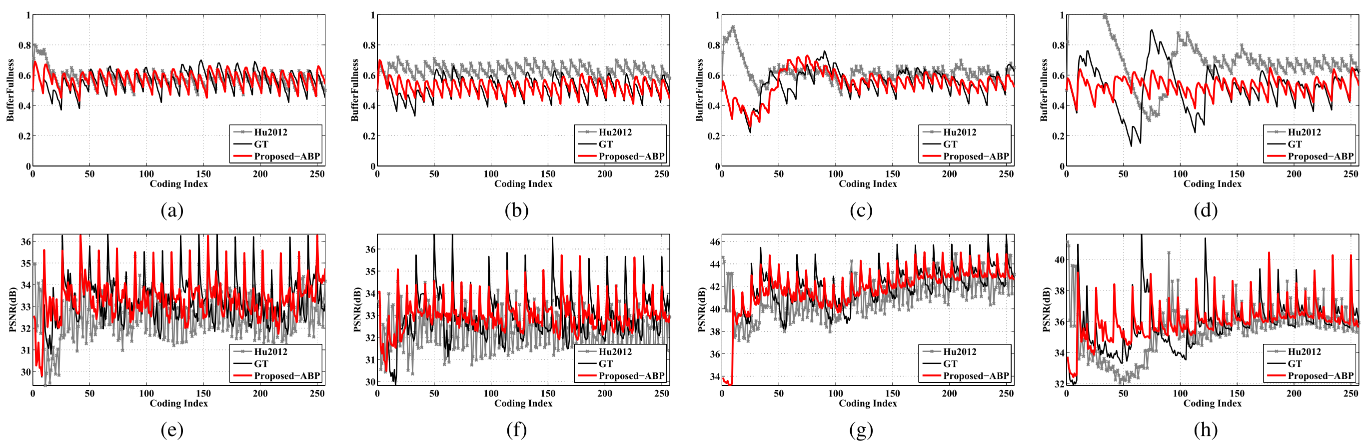

Fig. 6. Buffer Smoothness v.s. Quality Smoothness (GOP Size: 8). (a) Buffer Smoothness: "Harbour" (SL 0, 4CIF); (b) Buffer Smoothness: "Harbour" (SL 1, 4CIF); (c) Buffer Smoothness: "BQTerrace" (SL 0, HD); (d) Buffer Smoothness: "BQTerrace" (SL 1, HD); (e) Quality Smoothness: "Harbour" (SL 0, 4CIF); (f) Quality Smoothness: "Harbour" (SL 1, 4CIF); (g) Quality Smoothness: "BQTerrace" (SL 0, HD); (h) Quality Smoothness: "BQTerrace" (SL 1, HD).

as the criterion, denoted as STD.

$$\mathrm{STD}_s = \sqrt{\frac{1}{N_s}\sum_{j=1}^{N_s}(\mathrm{PSNR}_{j,s} - \frac{1}{N_s}\sum_{j=1}^{N_s}\mathrm{PSNR}_{j,s})^2}, \quad (29)$$

where $\mathrm{PSNR}_{j,s}$ is the PSNR value of the frame j in SL s. For each sequences, the results of average STD value for the comparative algorithms are also provided in Tables VI and VII. In most cases, our proposed algorithm with ABP setting has the smallest STD value among the one-pass RC schemes, especially for the GOP size 16. Comparing with the GT algorithm, our proposed algorithm with ABP setting can reduce the STD value from 0.23 to 0.35 dB in average. Comparing with the FixedQP algorithm, there is still some room to further improve the R-D performance. In the future, we will try to improve the R-D performance by further exploring the inter-layer information and designing an initial QP determination scheme.

V. Conclusion

In this paper, we propose a one-pass RC algorithm for spatial H.264/SVC based on the inner-layer bit allocation bargaining game. The inner-layer bit allocation is modeled as a bargaining game according to the constraints including bandwidth and buffer size. The inter-layer dependency relationship is exploited to enhance the prediction accuracy of R-D model. Then the bargaining powers are updated adaptively during the encoding process. At last, the proposed RC algorithm estimates the optimal QP for each frame based on the generalized NBS. The experimental results show that the proposed algorithm can achieve significantly gain as compared to other one-pass RC algorithms.

REFERENCES

[1] L. Xu, S. Kwong, H. Wang, Y. Zhang, D. Zhao, and W. Gao, "A universal rate control scheme for video transcoding," *IEEE Trans. Circuits Syst. Video Technol.*, vol. 22, no. 4, pp. 489–501, Apr. 2012.

[2] H. Schwarz, D. Marpe, and T. Wiegand, "Overview of the scalable video coding extension of the H.264/AVC standard," *IEEE Trans. Circuits Syst. Video Technol.*, vol. 17, no. 9, pp. 1103–1120, Sep. 2007.

[3] M. Wien, H. Schwarz, and T. Oelbaum, "Performance analysis of SVC," *IEEE Trans. Circuits Syst. Video Technol.*, vol. 17, no. 9, pp. 1194–1203, Sep. 2007.

[4] L. Xu, D. Zhao, X. Ji, L. Deng, S. Kwong, and W. Gao, "Window-level rate control for smooth picture quality and smooth buffer occupancy," *IEEE Trans. Image Process.*, vol. 20, no. 3, pp. 723–734, Mar. 2011.

[5] L. Xu, S. Kwong, Y. Zhang, and D. Zhao, "Low-complexity encoder framework for window-level rate control optimization," *IEEE Trans. Ind. Electron.*, vol. 60, no. 5, pp. 1850–1858, May 2013.

[6] S. Hu, H. Wang, S. Kwong, and C.-C. J. Kuo, "Novel rate-quantization model-based rate control with adaptive initialization for spatial scalable video coding," *IEEE Trans. Ind. Electron.*, vol. 59, no. 3, pp. 1673–1684, Mar. 2012.

[7] D. Pranantha, M. Kim, S. Hahm, B. Kim, K. Lee, and K. Park, "Dependent quantization for scalable video coding," in *Proc. IEEE Int. Conf. Adv. Commun. Technol.*, Feb. 2007, pp. 222–227.

[8] J. Liu, Y. Cho, Z. Guo, and C.-C. J. Kuo, "Bit allocation for spatial scalability coding of H.264/SVC with dependent rate-distortion analysis," *IEEE Trans. Circuits Syst. Video Technol.*, vol. 20, no. 7, pp. 967–981, Aug. 2010.

[9] Y. Liu, Z. G. Li, and Y. C. Soh, "Rate control of H.264/AVC scalable extension," *IEEE Trans. Circuits Syst. Video Technol.*, vol. 18, no. 1, pp. 116–121, Jan. 2008.

[10] L. Xu, W. Gao, X. Ji, and D. Zhao, "Rate control for hierarchical B-picture coding with scaling-factor," in *Proc. ISCAS*, May 2007, pp. 49–52.

[11] C.-W. Seo, J. W. Kang, J.-K. Han, and T. Q. Nguyen, "Efficient bit allocation and rate control algorithms for hierarchical video coding," *IEEE Trans. Circuits Syst. Video Technol.*, vol. 20, no. 9, pp. 1210–1223, Sep. 2010.

[12] *Joint Scalable Video Model JSVM 9.17 Software Package*, document CVS server for the JSVM software, Mar. 2009.

[13] A. Leontaris and A. M. Tourapis, *Rate Control for the Joint Scalable Video Model (JSVM)*, document JVT-W043, Video Team of ISO/IEC MPEG and ITU-T VCEG, San Jose, CA, USA, Apr. 2007.

[14] S. Hu, H. Wang, S. Kwong, T. Zhao, and C.-C. J. Kuo, "Rate control optimization for temporal-layer scalable video coding," *IEEE Trans. Circuits Syst. Video Technol.*, vol. 21, no. 8, pp. 1152–1162, Aug. 2011.

[15] S. Sanz-Rodriguez and F. Diaz-de-Maria, "RBF-based QP estimation model for VBR control in H.264/SVC," *IEEE Trans. Circuits Syst. Video Technol.*, vol. 21, no. 9, pp. 1263–1277, Sep. 2011.

[16] T. Ahmad and J. Luo, "On using game theory to optimize the rate control in video coding," *IEEE Trans. Circuits Syst. Video Technol.*, vol. 16, no. 2, pp. 209–219, Feb. 2006.

[17] J. Luo, I. Ahmad, and Y. Sun, "Controlling the bit rate of multi-object videos with noncooperative game theory," *IEEE Trans. Multimedia*, vol. 12, no. 2, pp. 97–107, Feb. 2010.

[18] X. Wang, S. Kwong, and Y. Zhang, "Applying game theory to rate control optimization for hierarchical B-pictures," *IEEE Trans. Broadcast.*, vol. 59, no. 4, pp. 591–601, Dec. 2013.

[19] H. Park and M. van der Schaar, "Bargaining strategies for networked multimedia resource management," *IEEE Trans. Signal Process.*, vol. 55, no. 7, pp. 3496–3511, Jul. 2007.

[20] J. F. Nash, Jr., "The bargaining problem," *Econometrica*, vol. 18, no. 2, pp. 155–162, Apr. 1950.

[21] N. Kamaci, Y. Altunbasak, and R. M. Mersereau, "Frame bit allocation for the H.264/AVC video coder via cauchy-density-based rate and distortion models," *IEEE Trans. Circuits Syst. Video Technol.*, vol. 15, no. 8, pp. 994–1006, Aug. 2005.

[22] T. Chiang and Y.-Q. Zhang, "A new rate control scheme using quadratic rate distortion model," *IEEE Trans. Circuits Syst. Video Technol.*, vol. 7, no. 1, pp. 246–250, Feb. 1997.

[23] D.-K. Kwon, M.-Y. Shen, and C.-C. J. Kuo, "Rate control for H.264 video with enhanced rate and distortion models," *IEEE Trans. Circuits Syst. Video Technol.*, vol. 17, no. 5, pp. 517–529, May 2007.

[24] L. Liu, X. Zhuang, Z. He, and Y. Sun, "H.264/AVC rate control with enhanced rate-quantisation model and bit allocation," *IET Image Process.*, vol. 5, no. 7, pp. 619–629, Oct. 2011.

[25] L. Liu and S. Zhuang, "A novel square root rate control algorithm for H.264/AVC encoding," in *Proc. ICME*, Jun./Jul. 2009, pp. 814–817.

[26] K. Binmore, *Fun and Games: A Text on Game Theory*. Lexington, MA, USA: D.C. Heath, 1991.

[27] Z. Li, F. Pan, K. P. Lim, G. Feng, X. Lin, and S. Rahardja, *Adaptive Basic Unit Layer Rate Control for JVT*, document JVT-G012-r1, 7th JVT meeting, Pattaya, Thailand, Mar. 2003.

[28] G. Bjøntegaard, *Calculation of Average PSNR Differences Between RD-Curves*, document VCEG-M33, Austin, TX, USA, Apr. 2001.

Xu Wang (S'11) received the B.S. degree from South China Normal University, Guangzhou, China, in 2007, the M.S. degree from Ningbo University, Ningbo, China, in 2010, and the Ph.D. degree from the Department of Computer Science, City University of Hong Kong, Hong Kong, in 2014. He is currently a Post-Doctoral Researcher with the Department of Computer Science/Shenzhen Research Institute, City University of Hong Kong. His research interests are video coding and stereoscopic image/video quality assessment.

Sam Kwong (M'93–SM'04–F'13) received the B.S. degree in electrical engineering from the State University of New York at Buffalo, Buffalo, NY, USA, in 1983, the M.S. degrees in electrical engineering from the University of Waterloo, Waterloo, ON, Canada, in 1985, and the Ph.D. degree from the University of Hagen, Hagen, Germany, in 1996. From 1985 to 1987, he was a Diagnostic Engineer with Control Data, Ltd., Toronto, ON. He joined Bell-Northern Research, Ottawa, ON, as a member of the scientific staff. In 1990, he became a Lecturer with the Department of Electronic Engineering, City University of Hong Kong, Hong Kong, where he is currently a Professor with the Department of Computer Science. His research interests are video and image coding and evolutionary algorithms.

Long Xu (M'12) received the M.S. degree in applied mathematics from Xidian University, Xi'an, China, in 2002, and the Ph.D. degree from the Institute of Computing Technology, Chinese Academy of Sciences, Beijing, China, in 2009. He was a Post-Doctoral Researcher with the Department of Computer Science, City University of Hong Kong, Hong Kong, and the Department of Electronic Engineering, Chinese University of Hong Kong, from 2009 to 2012. From 2013 to 2014, he held a post-doctoral position with the School of Compute Engineering, Nanyang Technological University, Singapore. He received the Honor of the 100 Talents Program of the Chinese Academy of Sciences. He is currently a Professor with the National Astronomical Observatories, Chinese Academy of Sciences. His research interests include image/video coding, image processing, machine learning, visual quality assessment, solar radio astronomy, and wavelet.

Yun Zhang (M'12) received the B.S. and M.S. degrees in electrical engineering from Ningbo University, Ningbo, China, in 2004 and 2007, respectively, and the Ph.D. degree in computer science from the Institute of Computing Technology, Chinese Academy of Sciences (CAS), Beijing, China, in 2010. From 2009 to 2014, he was a Visiting Researcher and a Post-Doctoral Researcher with the Department of Computer Science, City University of Hong Kong, Hong Kong. In 2010, he joined the Shenzhen Institutes of Advanced Technology at CAS. He has served as an Associate Professor since 2012. His research interests are 3D video coding, visual perception, and content-based video processing.